SCIENTIFIC REPORTS

OPEN

Size effects in Atomic-Level Epitaxial Redistribution Process of RuO_2 over TiO_2

Guolei Xiang[2], Xuejun Shi[1]*, Yulong Wu[1], Jing Zhuang[2] & Xun Wang[2]

[1]Institute of Nuclear and New Energy Technology, Tsinghua University, Beijing 100084, P. R. China, [2]Department of Chemistry, Tsinghua University, Beijing 100084, P. R. China.

SUBJECT AREAS:
SURFACE CHEMISTRY
NANOPARTICLES
CHEMICAL PHYSICS
INORGANIC CHEMISTRY

Received
14 August 2012

Accepted
12 October 2012

Published
9 November 2012

Correspondence and requests for materials should be addressed to Y.L.W. (wylong@tsinghua.edu.cn) or X.W. (wangxun@mail.tsinghua.edu.cn)

* Current address: Beijing Shenwu Environment & Energy Technology Corp, Beijing 102200, P. R. China

Controls over the atomic dispersity and particle shape of noble metal catalysts are the major qualities determining their usability in industrial runs, but they are usually difficult to be simultaneously realized. Inspired from the Deacon catalyst in which RuO_2 can form epitaxial layers on the surfaces of Rutile TiO_2, here we have investigated the shape evolution process of RuO_2 nanoparticles on the surface of P25 TiO_2. It is found that size effects exist in this process and RuO_2 nanoparticles with sizes ~sub-2 nm can be transformed into epitaxial layers while nanoparticles with bigger sizes are not apt to change their shapes. Based on a thermodynamic model, we infer such transformation process is jointly driven by the surface tension and interfacial lattice match between the nanoparticles and substrates, which may be suggestive for the design of noble metal catalysts integrating both active crystal planes and high atomic exposure ratios.

Shape-controlled synthesis of nanocrystals is a promising route to fully utilize their unique properties due to the exposure of specific crystalline facets, especially for catalyst materials[1–3]. Many methods have been developed to prepare highly efficient catalyst materials with reactive surfaces, which provide new views for the fields of catalysis science. Now it is possible to get various well-shaped noble metal nanocrystals as effective nanocatalysts, which can serve as ideal models to demonstrate academic conceptions.[4,5] However, further applications of these costly materials are usually limited either by their small BET surface areas or low exposure degree of the active compositions on the surfaces, because these well-shaped nanocrystals usually display relatively big sizes so that most of the noble metal atoms are hidden within the internal bulk phases. Loading catalytically active components on supports is an effective and industry-practicing method to increase the dispersity and stability of noble metal catalysts,[6,7] but it is usually unable to control the morphology of the catalyst nanoparticles, especially when their diameters are below 5 nm. So it would be much valuable to integrate simultaneous controls over the atomic dispersity and particle shape of noble metal catalysts.

It has been recognized that catalysts usually undergo shape transformation during reactions, which means that the nanometer-sized catalysts are not quite stable during reactions at high temperatures[8–11]. Actually many nanoparticles are thermally instable relative to their bulk phases because of the reduction in sizes and dimensions. In principle, such transformation behavior may be utilized as a treatment method to prepare reformed catalysts on substrates by designing the interactions on their interfaces. Previous reports showed that both the long-term catalytic activity and stability of RuO_2 could be maintained in catalytic HCl oxidation reactions (also known as Deacon reactions) if it formed epitaxial heterogeneous structures on the surfaces of rutile TiO_2 and SnO_2[12–15]. However, more efforts are still required to learn how this transformation process could occur (for example, the roles of the lattice structures of both catalysts and supports in this process and the underlying principle determining the shape transformation), which would be quite inspiring to the design of novel heterogeneous catalysts that integrate both active crystal planes and high atomic exposure ratios. Herein we have investigated the shape evolution process of RuO_2 nanoparticles on the surface of P25 TiO_2 under both catalytic reaction and direct thermal treatment conditions. We find that size effects exist in this process and the sub-2-nm nanoparticles of RuO_2 are more apt to transform into epitaxial layers with atomic thickness on the surfaces of P25 TiO_2 supports than those with bigger sizes. To reveal the mechanism, we further establish a thermodynamic model to analyze such transformation, based on which we infer that the epitaxial layer of RuO_2 over TiO_2 is much more stable than nanoparticles under the reaction conditions, and that it is surface tension and lattice-matched interfacial structure that co-drive the redistribution of RuO_2 from nanoparticles to epitaxial layers over TiO_2. It is also found that different from previous results[12,13,16,17], P25 is a better support for this process than pure rutile TiO_2 in that anatase particles in P25 serve as diluents to separate rutile and RuO_2 phases, resulting in the increase of the dispersity of the catalytically active RuO_2 components.

Results

To illustrate the shape transformation process of RuO_2 nanoparticles with different sizes, we started from studying their catalytic performances in HCl oxidation reactions (Deacon reaction)[16–20]. The reaction is a reversibly exothermic process, but high temperatures are usually required to increase the total reaction rates in industrial runs, which inevitably reduce the equilibrium conversion percentage of HCl. A relatively higher conversion rate above 90% can be realized below 300°C with lower HCl feed ratios according to the equilibrium conditions (see Figure S1)[18,21]. Here we investigate the reaction at 300°C with HCl feed ratio of 20% (the total pressure is 1 bar). In addition to P25-TiO_2, many other materials were also employed as supports to load RuO_2 as the Deacon catalysts, including SBA15, active carbon and various TiO_2. The conversion results of HCl are summarized in Figure 1a, where H and I denote the methods to prepare the supported RuO_2 catalysts via hydrothermal or impregnation method. It shows that RuO_2 catalyst supported on P25 via hydrothermal method (denoted as H-RuO_2/P25) displays the highest activity, compared with those supported on other materials, such as anatase, rutile, active carbon and SBA15. The theoretical HCl conversion percentage under the present operation conditions was calculated to be about 93% (Figure S1), and the present single-step conversion value is about 87% by H-RuO_2/P25, much higher than the results of SBA15 (61%), active carbon (40%), pure anatase (57%), rutile TiO_2 (54%) and I-RuO_2/P25 (77%), implying that P25 is a better support to load RuO_2 (It is different from the results in references in which rutile TiO_2 is a better support[16,17]. We will discuss it later).

We further focused on the RuO_2/P25-TiO_2 catalyst prepared by a hydrothermal method (denoted as H-P25 in Figure 1a, without calcination) to learn more insights into the catalytic process. We find that it is a self-enhanced catalytic process, during which both catalytic activities and stabilities are promoted. The reaction results over a period of 72 h are present in Figure 1b (H-P25). The conversion rate of HCl is relatively low during the first 8 h, but reaches a stable equilibrium state from 76% to 87% after 8 h. Then a stable state can be maintained at 87%, meaning both the activities and stabilities of RuO_2 catalysts are enhanced in the reaction, especially during the first 8 h.

To reveal the structural mechanism underlying the enhanced catalytic performances, we studied the evolution of RuO_2 nanoparticles on the surface of TiO_2 in detail through high-resolution transmission electron microscopy (HRTEM, Figures 2a–2c). Surfaces of the P25-TiO_2 supports are decorated with quite small particles (Figure 2a). In the amplified HRTEM image (Figure 2b), it can be seen that most of the nanoparticles are less than 2.0 nm in size. The existence of RuO_2 species on the surface of TiO_2 was further demonstrated by directly mapping each component on a high-resolution Z-contrast (atomic number Z) image, which was obtained on a 200 kV high angle annular dark-field scanning transmission electron microscope (HAADF-STEM). RuO_2 particles on the surface of TiO_2 can be directly visualized by the bright spots due to its higher Z-contrast (Figure 2c), also showing the uniform distributions over the supports.

Structural characterization results of the catalyst after 72-h reactions are shown in Figures 2d-2g and S2, which are quite different from the results before reaction. The initial particles of RuO_2 on the surfaces of TiO_2 disappeared after Deacon reactions (see Figures 2d and S2), implying the loss or redistribution of RuO_2. Given the fact that the color of RuO_2/P25 catalyst was still quite black and the activity was promoted and could be well kept, we concluded that RuO_2 was preserved during the reaction. The HAADF-STEM image (Figure 2e) shows that the surfaces of some TiO_2 particles are still quite bright, indicating RuO_2 is coated on the surface of the supports to form a kind of core-shell structure. Moreover, the element mapping images of Ti and Ru further prove the existence of RuO_2, because Ti mapping overlaps the whole profile of the selected area,

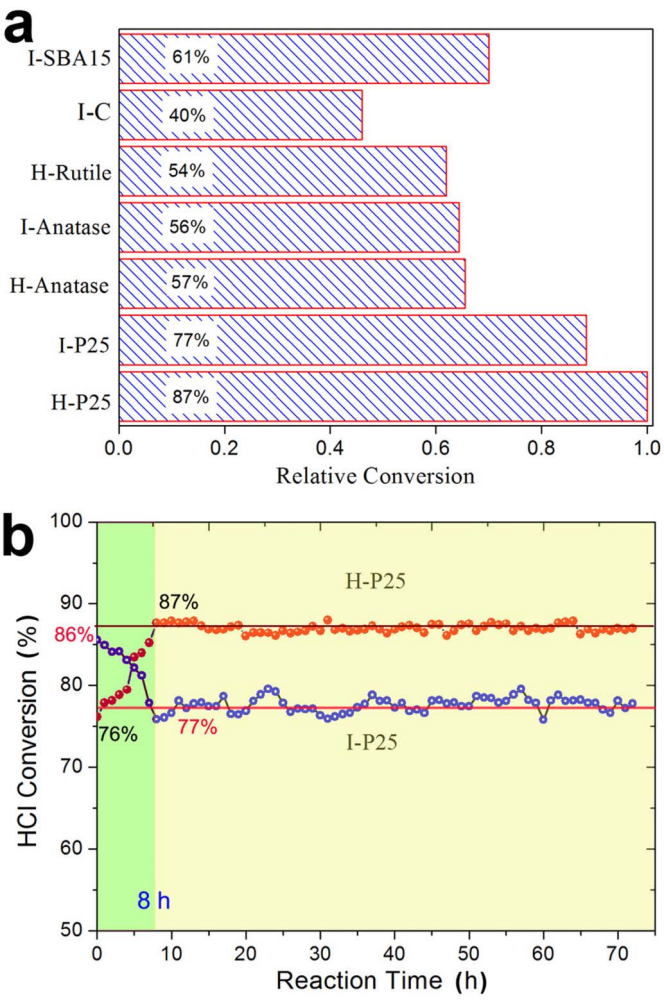

Figure 1 | (a) Relative activities of RuO_2-based catalysts on different supports indicated by the relative and absolute conversion of HCl gas. (b) Catalytic evolution of both activity and stability of RuO_2/P25 prepared via hydrothermal and impregnation methods over a period of 72 h.

while the imaging of Ru well corresponds to the bright parts in Figure 2e (Figures 2f–2g). So it is clear that RuO_2 nanoparticles underwent shape transformation to form epitaxial structure during Deacon reaction at 300°C, which promoted the catalytic activity and stability during the first 8 h due to the increased dispersion of RuO_2 over TiO_2.

The enhanced catalysis results also suggest that the epitaxial layer of RuO_2 over TiO_2 is more stable than the supported particles, and such acquired stability also indicates that TiO_2 can effectively stabilize RuO_2 on its surface. To learn more about the interfacial interactions, the catalyst after 72-h reaction was further characterized on a spherical aberration-corrected field-emission high-resolution transmission electron microscopy (SACFE-HRTEM) by forming lattice images of angstrom resolution. TEM results of a TiO_2 particle are present in Figures 2h and 2i, which clearly show the epitaxial island layer structure on the surface region. The phase of the substrate particle is identified to be rutile by measuring the lattice fringes. The lattice spacing of ~0.30 nm can be indexed to be the (110) facet of rutile TiO_2, therefore the exposing surface of the rutile nanoparticle can be determined to be (110), according to the tetragonal type lattice structure (inset in the Figure 2i). Thickness of the island epilayer is about 1.0 nm, and the oriented lattice spacing is measured to be 0.30 nm, in agreement with the (110) facet of RuO_2. So the above data suggest that an epitaxial growth layer was formed after the shape transformation of RuO_2, which can be expressed as (110)RuO_2//

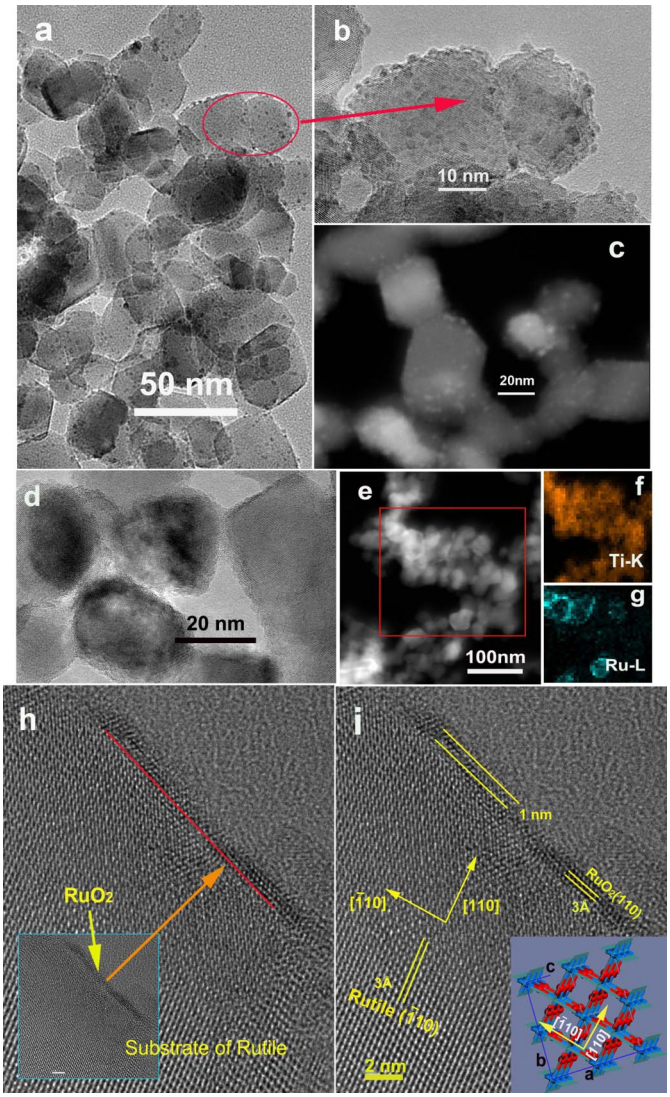

Figure 2 | Shape transformation of RuO_2 nanoparticles on the surface of P25 TiO_2. (a–b) low and high resolution TEM images showing the uniform loading of sub-2-nm RuO_2 nanoparticles on the surface of P25-TiO_2. (c) HAADF-STEM image showing the appearance of RuO_2 nanoparticles on TiO_2 surface. (d) TEM image showing the disappearance of the original RuO_2 nanoparticles. (e) HAADF-STEM image indicating that Ru element was preserved on the surface of TiO_2 by the bright contrast. (f–g) Element mapping results of Ti and Ru corresponding to the selected area in (e). (h) and (i) Spherical aberration-corrected high-resolution transmission electron microscopy images illustrating an epitaxial island of RuO_2 on the rutile(110) surface, with a thickness of ~1.0 nm. The inset in (f) is the orientation of rutile <110> directions.

(110)rutile-TiO_2. Such a result is not a casual event, but is dominated by the inherent structural matching between rutile and RuO_2, because they share the same type of lattice symmetry and almost the same lattice parameters (a=4.59 Å, c=2.96 Å for rutile and a=4.49 Å, c=3.10 Å for RuO_2). For epitaxial growth, the degree of lattice mismatch is the most important factor influencing the growth modes on the interface. The degree of lattice mismatch of RuO_2 on rutile (110) surface is determined to be 2.2%, within the limit for the epitaxial layer growth (<5%)[22], therefore it is quite reasonable for the appearance of RuO_2 island layer on rutile (110) surface.

According to the above analysis, we conclude that the self-enhanced catalytic performance of RuO_2 in the present Deacon reaction, including both activity and stability, is driven by its nearly lattice-matched epitaxial redistribution over rutile TiO_2 as illustrated in Figure 3a. The diagram describes the evolution from metastable nanoparticles to more stable epitaxial layers on substrates, which can promote the capability of the catalysts in reactions. Different from previous results[12,13,16,17], P25 is a better support for this process than pure rutile TiO_2. For the present P25-TiO_2 support, rutile particles can act as the real support for RuO_2 due to the matched lattice structure, while anatase particles mainly serve as diluents to separate rutile and RuO_2 phases, resulting in the increase of the dispersity of the catalytically active RuO_2 components. Such redistribution not only increases the effective surface area of catalytically active RuO_2 component, but also promotes the activity by forming specific facets induced by the rutile TiO_2 substrates, especially the active and stable RuO_2(110) surface[23–25]. Many efforts have been concentrated on revealing the catalytic oxidation reaction mechanisms of reducing gases over RuO_2(110) surface, such as CO, H_2, NH_3 and HCl[23,24,26–35]. On the stoichiometric RuO_2(110) surface, there are two kinds of coordinately unsaturated atoms (Figure 3b), namely the bridging oxygen atoms (O_{br}), which are coordinated only to two Ru atoms, and the 1f-cus-Ru atoms (Ru_{cus}) which are 1-fold coordinately unsaturated. These coordinately unsaturated atoms are the real catalytic active sites for the catalytic oxidations over RuO_2(110)[25,28]. So this is another factor accounting for the self-enhanced catalysis results due to the generation of specific RuO_2(110) planes through the epitaxial redistribution on the rutile surface after shape transformation.

Some similar coating structures of RuO_2 were also observed over other supports, such as rutile and SnO_2[12,15,19], and they were proposed to be caused by chlorination of RuO_2 catalysts during HCl oxidation reaction. In these processes, HCl, which was thought to be indispensable, acted as an inducer to enable the redistribution of RuO_2 due to

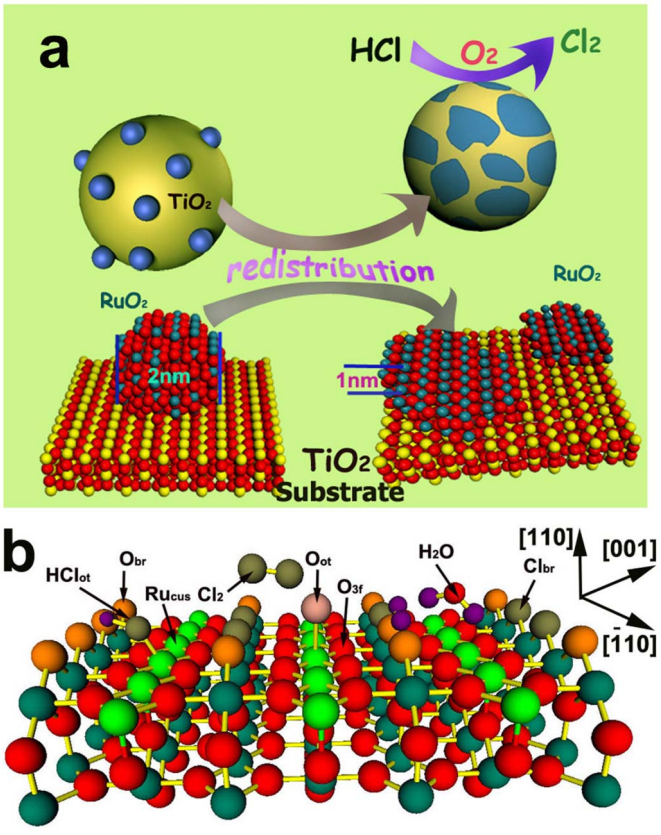

Figure 3 | (a) Schematic diagram illustrates the evolution of RuO_2 catalysts on the surface of TiO_2 from sub-2-nm nanoparticles to lattice-matched atomic-level epitaxial layer. (b) Mechanism of the Deacon reaction over RuO_2(110) surface based on well-studied DFT calculations.

the formation of $RuO_{2-x}Cl_x$ at the reaction temperature. Here we find that the redistribution of sub-2-nm RuO_2 nanoparticles can also be realized only by heat treatment in the absence of HCl, and the transformation is size-dependent. The shape transformation results by calcining the catalysts at 400°C for 10 h in air are shown in Figures 4a–c. From the STEM image we can see that the RuO_2 nanoparticles initially loaded on the surface of TiO_2 disappear after heat treatment, and obvious epilayers form on the surfaces (Figure 4a). The elemental mapping data of Ti-K and Ru-L electrons also verify the coating structure of RuO_2 over P25 TiO_2 (Figure 4b and 4c).

Further control experiments were contrasted with the catalyst prepared via an impregnation method (I-RuO_2/P25), which was calcined at 400°C to form RuO_2 before reaction. It can be seen that the catalyst particles are larger than those in Figure 2a, and they don't tightly adhere to the supports as shown in Figure 4d and S3. Even after treating at 400°C, the products are still particles rather than epitaxial layers, meaning these particles were not apt to change their shape as the sub-2-nm particles did. Such a structure feature can be reflected by its performance in Deacon reactions as shown in Figure 1b (I-P25). There is also an evolution process of activity and stability, but negative. The conversion percentage of HCl decreases from 86% to 77% during the first 8 h. We find there was also a shape transformation process of from particles to layers for I-RuO_2/P25 after Deacon reaction as displayed in Figure 4e, but they are not quite uniformly coated over TiO_2. It is apparent that the larger sizes of the initial nanoparticles cannot lead the atomic dispersion state of the RuO_2 active components on the surface of the P25. Additionally, this result also confirms the roles of HCl in the process, which agree with the results from literatures.

Discussion

The above results suggest that the redistribution of sub-2-nm RuO_2 nanoparticles can be realized either by Deacon reactions or direct heat treatment without HCl. Such a shape transformation is a thermodynamically spontaneous process, because the supported sub-2-nm nanoparticles are not so stable as the epitaxial layer. The difference actually deals with one of most fundamental problems with nanoscience, namely the stability of ultrafine nanoparticles of different shapes on substrates, and herein they are the supported particles and epilayers as illustrated in Figure 5a and 5b. When the dimensions are restricted within nanoscale, surface tension becomes the most important factor that dominates most physicochemical properties of nanomaterials, especially the interface behaviors and surface stability. Based on the analysis, we establish a qualitatively theoretical model to analyze the difference by considering the factors causing free energy change (Figure S4). At a certain temperature when the atoms can overcome the constraints from lattice by acquiring enough vibration energy from the environment, mainly through the injection of heat, catalyst particles will become instable by leaching atoms into the environment or undergoing shape change due to surface relaxation. It is the inverse process of crystallization, also controlled by the interfacial tension γ. In an equilibrium state transition process for spherical particles, the free energy change ΔG can be expressed as

$$\Delta G = \left(\frac{4\pi r^3 \Delta G_v}{3} - 4\pi r^2 \gamma_e\right) f(\theta) \quad (1)$$

$$f(\theta) = (1 - \cos\theta)^2 (2 + \cos\theta)/4 \quad (2)$$

where ΔGv is the free energy change of the transformation per unit volume and f(θ) is the angular factor[22,36].

The diagram of $\Delta G/f(\theta)$ is displayed in Figure 5c, which refers to a size reduction process from a larger crystal grain. It shows that the surface tension acts as the major force that determines the thermal stability of epitaxial nanoparticles when their sizes are close to nuclei. If the atoms acquire enough vibration energy in a particle that is close to the critical size (r^*), spontaneous shape transformation occurs and the tendency will be further intensified by the shrinking grain size. Finally the whole particle completely vanishes, and this is the reason why we could not find residual RuO_2 particle on the surface of TiO_2 after heat treatment or Deacon reactions.

On the other hand, because the degree of lattice mismatch between rutile and RuO_2 is about 2.2%, it is possible to form epitaxial layers on the interfaces just as we have observed in Figures 2 and 4. Therefore the contact angle disappear (that is θ=0) as shown in Figures 5b, meaning the interfacial tension between them is nearly zero (γ_s-$\gamma_e \approx 0$). The actual zero contact angle further reflects the most stable heterogeneous growth mode for RuO_2 on the surface of rutile TiO_2 is the layer growth. The effect of particle shapes on the thermal stability of RuO_2 over TiO_2 can be further interpreted in terms of the angular factor $f(\theta)$. It clearly indicates the inevitability for RuO_2 to transform from particles to atomic-level epitaxial layers. Dependence of the stability upon particle shapes (expressed by the contact angle θ) is illustrated in Figure 5d, expressed by ΔG along with f(θ) in the inset. It shows the thermodynamically instable tendency of the supported nanoparticles dramatically increases with increased contact angles. There is not any obvious driving force for the lattice-matched epitaxial layer, because ΔG for such structure is almost zero, thus the surface layer can be well stabilized by the substrate lattice. Therefore, we can say that the ultrafine RuO_2 nanoparticles, sub-2-nm in our system, are thermodynamically metastable; while TiO_2 can serve as an effective substrate to stabilize RuO_2 by forming epitaxial heterostructures. The two factors co-drive the shape transformation of RuO_2 catalysts from sub-2-nm nanoparticles to epitaxial layer on the surface of TiO_2, and the redistribution process further promotes its performances in catalytic reaction.

In summary, we have demonstrated an approach to enhance both the activity and stability of heterogeneous catalysts through lattice-matched atomic-level epitaxial redistribution over the supports. The shape transformation of RuO_2 from sub-2-nm nanoparticles to epilayer over TiO_2 was co-driven by thermal instability and interfacial

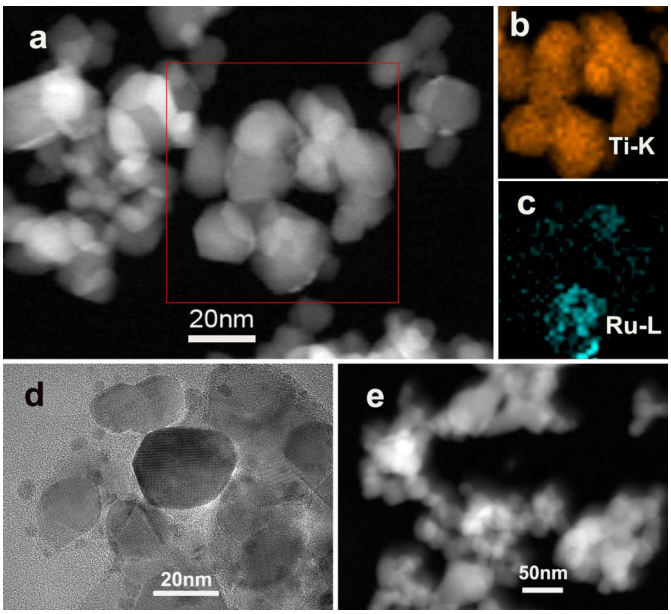

Figure 4 | Redistribution of RuO_2 nanoparticles by direct heat treatment at 400°C in the absence of HCl. (a) STEM image showing the epitaxial layers of sub-2-nm RuO_2 formed on the surface of TiO_2. (b) and c) are the element mapping data of the selected area in d), showing the coating structure of RuO_2 over P25. (d) TEM image of RuO_2 catalyst prepared via impregnation method after treated at 400°C. (e) STEM image of RuO_2 catalyst prepared via impregnation method after Deacon reaction.

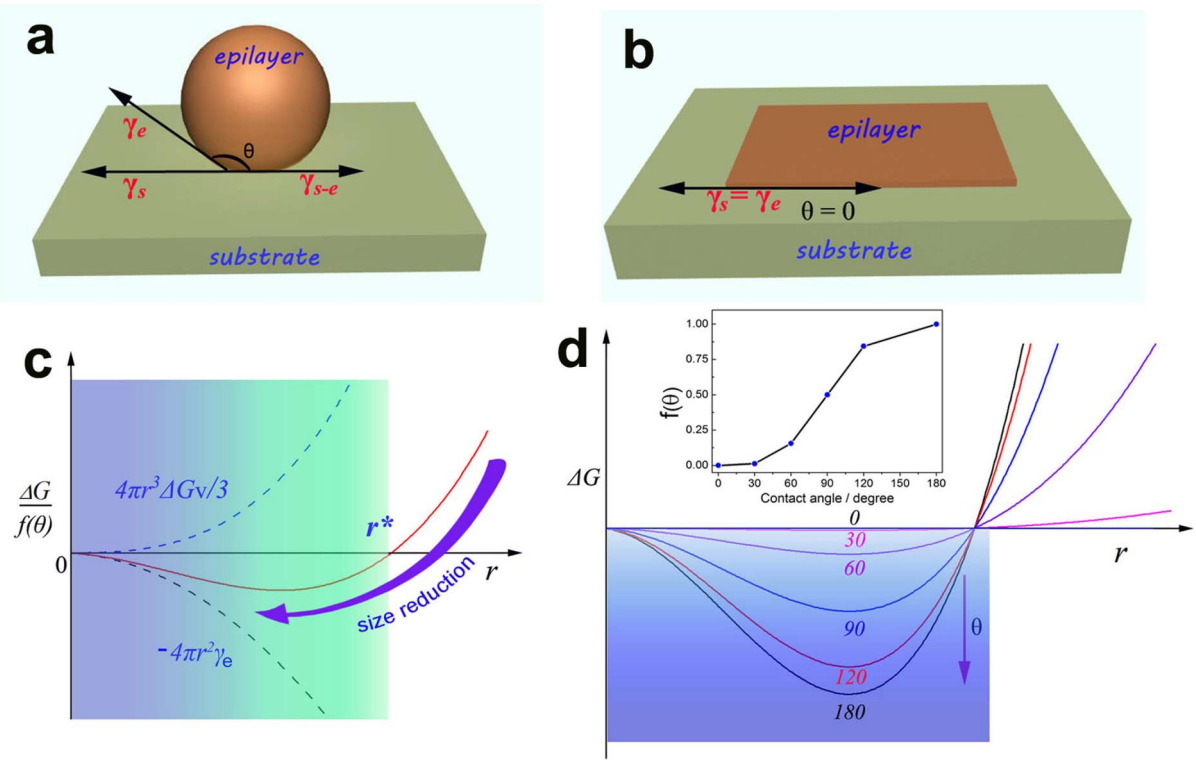

Figure 5 | Mechanism analysis of the stability of RuO_2 nanostructures on the surface of TiO_2. (a), Interfacial tensions at the boundary between TiO_2 substrate and RuO_2 epitaxial nanoparticle with a large contact angle, modeling the surface structure of the initial catalyst prepared via hydrothermal method. (b), Surface structure of lattice-matched RuO_2 epilayer on the surface of TiO_2, where the surface tension of the substrate (γ_s) is approximately equal to that of the epilayer (γ_e) because of the high degree of lattice match between RuO_2 and rutile. (c), Free energy diagram for the phase transition of a nanoparticle explaining the instability of sub-2-nm RuO_2 catalyst. (d), Effect of particle shape on the phase transition tendency of epitaxial layers on substrates expressed by the varied free energy change (ΔG). The inset is the diagram of angular factor $f(\theta)$, the function of contact angle that depicts the equilibrium particle shape on a substrate.

lattice match at high reaction temperatures, concluded by comparing the stability of surface heterostructures with different shapes on substrates. Improved catalytic activity and stability in the HCl oxidation reaction were realized to show the advantages of the process. The idea illustrated in the work may be suggestive for the design of noble metal catalysts integrating both active crystal planes and high atomic exposure ratios.

Methods

Preparation of catalysts. The RuO_2 catalysts employed in the work are 6% in weight loaded on various supporters, including TiO_2 (Degussa P25, anatase and rutile), active carbon and mesoporous SiO_2 SBA-15. $RuCl_3 \cdot 3H_2O$ was used as the RuO_2 precursor.

Hydrothermal method: To prepare supported RuO_2 catalysts via hydrothermal method, $RuCl_3 \cdot 3H_2O$ and supporters (P25, anatase and rutile) were mixed in ratio (6% RuO_2) using water as the solvent and reacted at 150°C for 10 h to get RuO_2. The products were separated by centrifugation and washed with water.

Impregnation method: Catalyst supporters (P25, anatase, active carbon and SBA-15) were soaked in the 0.1 $molL^{-1}$ HCl solutions containing $RuCl_3$ at a pH value of 4.5 and then stirred for 5 h. After separation, the powders were dried at 130°C, then heated at 180°C for 8 h and calcined at 400°C for another 8 h.

Catalyst characterization. Morphologies of the products were investigated on a high-resolution transmission electron microscopy (HRTEM) of FEI Tecnai F20 with an accelerating voltage of 200 kV and FEI Tecnai G2 F20 S-Twin working at 200 kV.

Catalytic activity tests. The catalytic oxidation of HCl over supported RuO_2 was evaluated in a U-shaped reactor using 400 mg catalysts (sieve fraction 200–300 μm). At 300°C, during the reactions, hydrogen chloride and oxygen were used with a feed ratio of 20 vol% HCl: 80 vol% O_2. Each gas was introduced into the reactor by means of digital mass-flow controllers. The reaction conditions were set as a total pressure of HCl and O_2 mixture at 1 bar and a weight-hourly space velocity (WHSV) of 7500 $ml \cdot g^{-1} \cdot h^{-1}$. The materials of all the lines in the set-up were Teflon® in order to prevent from corrosion by HCl and Cl_2, particularly the downstream parts of the reaction system. The expellant gas was absorbed by ultrapure water and the conversion rate of HCl was calculated according to the changing conductivity of the ultrapure water. The final tail gas was absorbed using NaOH solution.

1. Xia, Y. N., Xiong, Y. J., Lim, B. & Skrabalak, S. E. Shape-Controlled Synthesis of Metal Nanocrystals: Simple Chemistry Meets Complex Physics? *Angew. Chem. Int. Edit.* **48**, 60–103 (2009).
2. Yang, H. G. *et al.* Anatase TiO_2 single crystals with a large percentage of reactive facets. *Nature* **453**, 638–642 (2008).
3. Habas, S. E., Lee, H., Radmilovic, V., Somorjai, G. A. & Yang, P. Shaping binary metal nanocrystals through epitaxial seeded growth. *Nat. Mater.* **6**, 692–697 (2007).
4. Tian, N., Zhou, Z. Y., Sun, S. G., Ding, Y. & Wang, Z. L. Synthesis of tetrahexahedral platinum nanocrystals with high-index facets and high electro-oxidation activity. *Science* **316**, 732–735 (2007).
5. Pan, J., Liu, G., Lu, G. M. & Cheng, H. M. On the True Photoreactivity Order of {001}, {010}, and {101} Facets of Anatase TiO2 Crystals. *Angew. Chem. Int. Edit.* **50**, 2133–2137 (2011).
6. Corma, A. From microporous to mesoporous molecular sieve materials and their use in catalysis. *Chem. Rev.* **97**, 2373–2419 (1997).
7. Valden, M., Lai, X. & Goodman, D. W. Onset of catalytic activity of gold clusters on titania with the appearance of nonmetallic properties. *Science* **281**, 1647–1650 (1998).
8. Tao, F. & Salmeron, M. In Situ Studies of Chemistry and Structure of Materials in Reactive Environments. *Science* **331**, 171–174 (2011).
9. Tao, F. *et al.* Reaction-Driven Restructuring of Rh-Pd and Pt-Pd Core-Shell Nanoparticles. *Science* **322**, 932–934 (2008).
10. Nolte, P. *et al.* Reversible Shape Changes of Pd Nanoparticles on MgO(100). *Nano Lett.* **11**, 4697–4700 (2011).
11. Nolte, P. *et al.* Shape changes of supported Rh nanoparticles during oxidation and reduction cycles. *Science* **321**, 1654–1658 (2008).
12. Seki, K. Development of RuO_2/Rutile-TiO_2 Catalyst for Industrial HCl Oxidation Process. *Catal. Surv. Asia.* **14**, 168–175 (2010).
13. Mondelli, C., Amrute, A. P., Krumeich, F., Schmidt, T. & Perez-Ramirez, J. Shaped RuO_2/SnO_2-Al_2O_3 Catalyst for Large-Scale Stable Cl_2 Production by HCl Oxidation. *Chemcatchem* **3**, 657–660 (2011).
14. Perez-Ramirez, J. *et al.* Sustainable chlorine recycling via catalysed HCl oxidation: from fundamentals to implementation. *Energy Environ. Sci.* **4**, 4786–4799 (2011).

15. Teschner, D. *et al.* An integrated approach to Deacon chemistry on RuO2-based catalysts. *J. Catal.* **285**, 273–284 (2012).
16. Deacon, H. Improvement in the Manufacture of Chlorine. U.S. Patent 85,370 patent (1868).
17. Deacon, H. U. S. Patent 165,802 patent (1875).
18. Arnold, C. W. & Kobe, K. A. Thermodynamics of the Deacon Process. *Chem. Eng. Prog.* **48**, 293–296 (1952).
19. Iwanaga, K. *et al.* The Development of Improved Hydrogen Chloride Oxidation Process. *Sumitomo Kagaku* **I**, 4–12 (2004).
20. Itoh, H., Kono, Y., Ajioka, M., Takezaka, S. & Katzita, M. U. S. Patent 4,803,065 patent (1989).
21. Zhi-Tao, C., Ming-Han, H., Fei, W. & Yong, J. Production Process of Chlorine from HCl by Catalytic Oxidation. *Chin. J. Proc. Eng.* **8**, 937–940 (2008).
22. Herman, M. A., Richter, W. & Sitter, H. *Epitaxy: Physical Principles and Technical Implementation.* (Springer, 2004).
23. Over, H. *et al.* Atomic-scale structure and catalytic reactivity of the RuO_2(110) surface. *Science* **287**, 1474–1476 (2000).
24. Lopez, N., Gomez-Segura, J., Marin, R. P. & Perez-Ramirez, J. Mechanism of HCl oxidation (Deacon process) over RuO_2. *J. Catal.* **255**, 29–39 (2008).
25. Over, H. Surface Chemistry of Ruthenium Dioxide in Heterogeneous Catalysis and Electrocatalysis: From Fundamental to Applied Research. *Chem. Rev.* (2012).
26. Wang, J. H. *et al.* Surface coordination chemistry: Dihydrogen versus hydride complexes on RuO_2(110). *Angew. Chem. Int. Edit.* **42**, 2151–2154 (2003).
27. Knapp, M., Crihan, D., Seitsonen, A. P. & Over, H. Hydrogen transfer reaction on the surface of an oxide catalyst. *J. Am. Chem. Soc.* **127**, 3236–3237 (2005).
28. Crihan, D. *et al.* Stable deacon process for HCl oxidation over RuO_2. *Angew. Chem. Int. Edit.* **47**, 2131–2134 (2008).
29. Wang, C. C., Yang, Y. J., Jiang, J. C., Tsai, D. S. & Hsieh, H. M. Density Functional Theory Study of the Oxidation of Ammonia on RuO_2(110) Surface. *J. Phys. Chem. C* **113**, 17411–17417 (2009).
30. Jacobi, K., Wang, Y. & Ertl, G. Interaction of hydrogen with RuO_2(110) surfaces: Activity differences between various oxygen species. *J. Phys. Chem. B* **110**, 6115–6122 (2006).
31. Seitsonen, A. P. & Over, H. Oxidation of HCl over TiO_2-Supported RuO_2: A Density Functional Theory Study. *J. Phys. Chem. C* **114**, 22624–22629 (2010).
32. Zweidinger, S. *et al.* Reaction mechanism of the oxidation of HCl over RuO_2(110). *J. Phys. Chem. C* **112**, 9966–9969 (2008).
33. Knapp, M. *et al.* Complex interaction of hydrogen with the RuO_2(110) surface. *J. Phys. Chem. C* **111**, 5363–5373 (2007).
34. Jacobi, K. & Wang, Y. M. Interaction of NO with the O-rich RuO_2(110) surface at 300 K. *Surf. Sci.* **603**, 1600–1604 (2009).
35. Wendt, S., Knapp, M. & Over, H. The role of weakly bound on-top oxygen in the catalytic CO oxidation reaction over RuO_2(110). *J. Am. Chem. Soc.* **126**, 1537–1541 (2004).
36. Mullin, J. W. *Crystallization.* (Butterworth-Heinemann, 2001).

Acknowledgements

This work was supported by NSFC (91127040, 20921001, 21176142), the State Key Project of Fundamental Research for Nanoscience and Nanotechnology (2011CB932402), and the National High Technology Research and Development Program of China (2008AA06Z342).

Author contributions

G. L. X. and X. J. S. contributed equally to this work. G. L. X. performed the synthesis and structural characterization of the catalysts. X. J. S. tested the catalytic performances and processed the data. J. Z. contributed to the characterization process. X. W. and Y. L. W. conceived and designed the experiments, and are responsible for the work. All authors discussed the results, wrote and commented on the manuscript.

Additional information

Supplementary information accompanies this paper at http://www.nature.com/scientificreports

Competing financial interests: The authors declare no competing financial interests.

How to cite this article: Xiang, G., Shi, X., Wu, Y., Zhuang, J. & Wang, X. Size effects in Atomic-Level Epitaxial Redistribution Process of RuO_2 over TiO_2. *Sci. Rep.* **2**, 801; DOI:10.1038/srep00801 (2012).